Received: 22 September 2023 | Revised: 16 November 2023 | Accepted: 20 November 2023 | Published online: 22 November 2023

RESEARCH ARTICLE

Magnetic Field Sensing by Magnetic-Fluid-Coated Capillary Long-Period Fiber Gratings

Journal of Optics and Photonics Research
yyyy, Vol. XX(XX) 1–5
DOI: 10.47852/bonviewJOPR32021778

BON VIEW PUBLISHING

Mengjiao Ding[1], Mengxue Tang[1], Ziyang Hua[1], Xin Wang[1] and Yunhe Zhao[1,*]
1 Institute of Logistics Science and Engineering, Shanghai Maritime University, China

Abstract: In this paper, we presented and experimentally investigated a novel magnetic field sensor based on magnetic-fluid (MF)-coated capillary long-period fiber gratings (CLPFGs). The CLPFGs with short length of no more than 10 mm and period of 1 mm were fabricated by point-to-point arc discharge method, and then infiltrated in an MF-filled glass tube forming a packaged MF-coated CLPFGs magnetic field sensors. A redshift in resonances of CLPFGs was brought out after packaging process, due to external refractive index changing. With the increasing external magnetic field, the intensity of resonant dips gradually decreased, which is caused by magnetostrictive effect together with refractive index variations. Moreover, CLPFGs with the same grating period and different grating lengths were comparatively investigated and analyzed. The resonant dips with larger transmissive depth present faster descend to the external magnetic field, result in higher sensitivity. The sensitivity of 0.036 dB/Oe could be obtained, when the CLPFGs has a grating length of 9 mm. What is more, the sensor is insensitive to temperature which can avoid the effect of temperature. The proposed MF-coated CLPFGs magnetic field sensor has potential applications in magnetic field systems.

Keywords: long period fiber grating, optical fiber sensing, magnetic field sensor, magnetic fluid

***Corresponding author:** Yunhe Zhao, Institute of Logistics Science and Engineering, Shanghai Maritime University, China. Email: yhzhao@shmtu.edu.cn

1. Introduction

Recently, magnetic field sensor (MFS) has played an increasingly important role in biomedical testing, aerospace industry space, and geophysical research (Murzin et al., 2020; Hadjigeorgiou et al., 2021; Poliakov t al., 2017). The conventional electric MFSs are mostly based on the sensing principles such as Hall effect (Roy et al., 2020), magnetoresistive effect (Wang et al., 2018) and fluxgate (Hsieh & Chen, 2021). Fiber-optic MFSs outperform the electric MFSs, because it is light in weight, small in size, low in cost and can be remotely controlled. Nowadays, fiber-optic MFSs are mainly based on Faraday effect (Mihailovic & Petricevic, 2021) and magnetostrictive materials (Yang et al., 2009). However, it is difficult to integrate magnetostrictive materials with optical fibers in some cases. At present, fiber-optic MFSs based on magneto-optical-effect have drawn increasing amounts of attention, among which magnetic fluid (MF) has been widely used as a sensitive component for magnetic field detection. The MF-based fiber-optic MFSs have good temperature stability and optical stability, which can maintain stable performance over a wide temperature range and is not easily affected by external interference. Moreover, the sensing element of the MF-based fiber-optic MFSs is composed of MF and optical fiber, without mechanical components, so it has a long lifespan.

Different types of MF-based fiber-optic MFSs have been proposed, such as grating-based sensors including Fiber Bragg grating (FBG) (Bao et al., 2018), tilted FBG (Yang et al., 2014), long-period fiber gratings (LPFGs) (Tang et al., 2015), and interferometric sensors such as Fabry Perot interferometer (FPI) (Zheng et al., 2017), Mach-Zehnder interferometer (MZI) (Luo et al., 2018), Michelson interferometer (Deng et al., 2013) and Sagnac interferometer (Alberto et al., 2018). Hollow core fiber (HCF), due to large refractive index difference between the cladding and hollow core, has been developed in magnetic field sensing fields. By utilizing the magneto-volume effect, the magnetic field sensitivity of FPI-based MFS is greatly improved (Wang et al., 2021). Using the U-shaped HCF, simultaneous measurement of magnetic field and temperature could be achieved

(Xu et al., 2022). An MZI-based MFS is formed, with interference between the LP_{01} and LP_{11} modes in HCF, which can achieve a higher sensitivity (Tian et al., 2022). Moreover, magnetic field sensing measurement could be realized by connecting the corroded HCF to the taper fiber which produces a whispering gallery mode resonance spectrum (Zhang et al., 2020). Apart from the above structures, the grating-based MFSs have also aroused great interest. Using the tapered FBG, the MFS can achieve intensity-modulated and large bandwidth measurement (Li et al., 2020). A vector MFS can be achieved by sealing the eccentric FBG into an MF-infiltrated glass capillary (Zhang et al., 2022). LPFGs has the advantages of the simplicity of configuration measurement and higher sensitivity. Based on MF-coated LPFGs within a standard single-mode fiber (SMF), the transmission minimum of the MFS is highly sensitive to the change of ambient medium (Zhang et al., 2015). The dispersion turning point based LPFGs can achieve a magnetic field sensitivity of 1.9 nm/mT, the temperature sensitivities was measured to be 1.56 nm/°C (Lu et al., 2022). For the tapered-LPFGs, the two resonant wavelengths exhibit responsive differences in magnetic field and temperature (Shao wt al., 2023). However, most LPFGs-based MFSs are easily affected by temperature. Therefore, it is important to eliminate temperature interference for LPFGs-based MFSs. A cascaded fiber structure comprising of MF-infiltrated micro-tapered LPFGs and FBG can solve the cross-sensitivity for temperature (Guo et al., 2023). In our previous work, a novel fiber sensor based on arc-induced LPFGs in capillary (CLPFGs) has been demonstrated, with advantages of low cost and good flexibility. Moreover, CLPFGs presents temperature insensitive behaviors (Zhao et al., 2023).

In this paper, we present a magnetic field sensing by MF-coated CLPFGs. The arc-discharged CLPFGs were immersed with MF, and then packaged in a glass tube. Experimental discussion is done on how the suggested sensor responds to the strength of external magnetic field. When magnetic field intensity changes, the intensity of resonant dip changes accordingly. The CLPFGs with different grating lengths of 8.5mm,9 mm and 10mm, have been studied comparatively. When the grating length was 9 mm, the magnetic field sensitivity could achieve 0.036dB/Oe. Moreover, the temperature disturbance has little influence on the magnetic field sensor. The presented MF-coated CLPFGs provide potential application prospects in magnetic field sensing.

2. Methodology

2.1. Design and principle

Figure 1
Schematic diagram of MF-coated CLPFGs

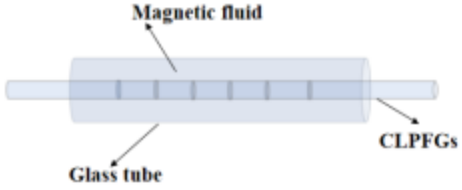

Figure 1 displays the schematic representation of CLPFGs with MF coatings. MF is a type of unique nano intelligent material whose rheological characteristics are changed hinging upon the strength of applied magnetic field. Besides, MF has obvious magneto-optical effect. For MF, solid magnetic particles will group together when an external magnetic field is present. As the magnetic field intensity changes, the refractive index of the MF can be expressed as (Guo et al., 2023):

$$n_{MF} = [n_s - n_b]\left[coth\left(\alpha\frac{H - H_{c,n}}{T}\right) - \frac{T}{\alpha(H - H_{c,n})}\right] + n_b \quad \#(1)$$
$$for\ H > H_{c,n}$$

Where $H_{c,n}$ is the critical magnetic field intensity depending on the type of carrier fluid and the volume concentration of nanoparticles, α corresponds to a fitting coefficient, and n_b and n_s are the initial and saturation values of n_{MF}, respectively.

The coupling mechanism of LPFGs is the coupling between forward transmitted core fundamental mode and forward transmitted cladding mode, when light propagates in the LPFGs, the periodic refractive index grating structure produces resonance attenuation in the spectrum (Zhang et al., 2015). In addition, the transmission minimum or resonance dip of the LPFGs is a function of the coupling constant κ and the grating length L (Konstantaki et al., 2011), which can be defined as:

$$T = cos^2(\kappa L) \quad (2)$$

The coupling constant κ decreases with the increase of external disturbances such as ambient refractive index, bending and lateral load. Using MF as the environmental medium for CLPFGs, coating it on the outside of the grating structure. When applying external magnetic field, magnetohydrodynamic nanoparticles wrapped on the CLPFGs grating structure are magnetized, resulting in a magnetostrictive effect, which in turn causes the axial strain of the CLPFGs (Wang & Chiang, 2015).

2.2. Fabrication and measurement setup

In experiment, the CLPFGs have been fabricated using arc-discharged method as our previous work (Zhao et al., 2023). The Fe_3O_4 MF (EMG605 Ferro Tec) used in this experiment has a volume fraction of 3.6% of magnetic particles, the diameter of magnetic particles suspended in base solution is about 10 nm. The refractive index of the MF is estimated to be around 1.40 without external magnetic field. When the intensity of the external magnetic field increases, particles gather in the direction of the magnetic field, forming columnar or chain like structures in the liquid (Konstantaki et al., 2011). Figure 2(a) displays packing procedure of the sensor. First, we inserted the fabricated CLPFGs grating structure into a glass tube which has an inner diameter of 1mm, adjusted the position of the glass tube to ensure coverage of the grating area, and then fixed the sensor. Because of the viscosity of the magnetic fluid material, we used a syringe with a needle tubing inner diameter of 0.1 mm to inject the MF from one end of the glass tube. Finally, for purpose of preventing the volatilization and leakage of the MF, ultraviolet (UV) glue is utilised to seal both ends of the glass tube, and the UV light is used to accelerate the solidification of the glue. Figure 2(b) shows the image of the packaged MF-coated CLPFGs. The total length of the packaged MF-coated CLPFGs is ~ 4 cm.

Figure 2
(a) Schematic diagram of sensor packaging experimental device (b) Image of packaged magnetic field sensor

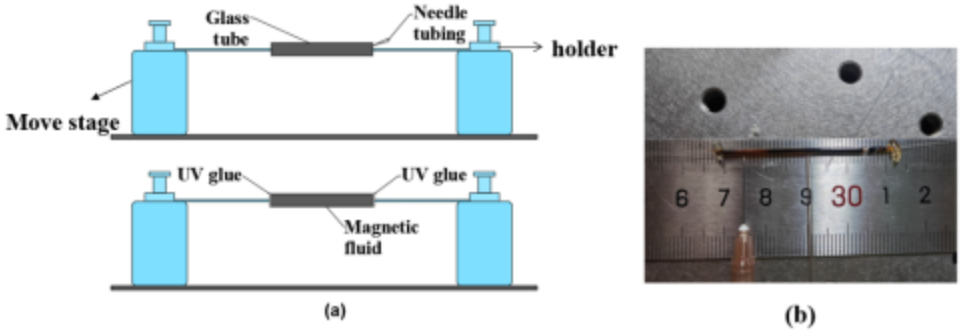

A magnetic field sensing system was created to look into the projected capabilities of CLPFGs for magnetic field sensing. Figure 3 displays the schematic diagram of experimental setup for measuring magnetic fields, which mainly include a broadband light source (BBS, SC-5, YSL), an optical spectrum analyzer (OSA, AQ6317B, ANDO), a tesla meter, a pair of electromagnets, and a current source. The MF-coated CLPFGs sensor is placed vertically between the magnetic poles of two electromagnets. The magnetic field strength created in region could be continually modified by modifying generating current, and to observe the magnetic field timely, the sensor of tesla meter can be placed as close as possible to the area to be measured. At room temperature, the light emitted by the BBS is transmitted to the grating area covered by a magnetic field, and then connected to the OSA through an output SMF to obtain spectral performance.

Figure 3
Schematic diagram of experimental setup for magnetic field sensing

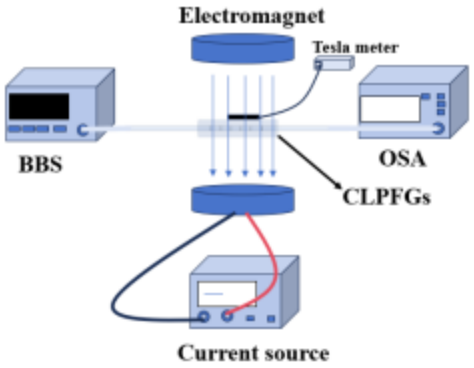

3. Results and Analysis

The magnetic field sensing characteristics of MF-coated CLPFGs were tested at room temperature. At first, we measured the magnetic field sensing response of the bare CLPFGs with length of 8.5 mm, which has two resonant dips (dip A and dip B) at 1378.4 nm and 1483.8 nm, respectively, as shown in the Figure 4 (a). We measured the magnetic field sensing response of the sensor when it was not encapsulated by MF, with the magnetic field changing from 150Oe to 500 Oe, the resonant dip A and dip B exhibit magnetic field sensitivity of 0.0009dB/Oe and -0.001dB/Oe, respectively, as show in the insertion of Figure 4 (a). Before the packaging, the sensor was insensitive to magnetic fields. Figure 4(b) illustrated the spectra of CLPFGs with a grating length of 8.5mm before and after MF packaged, and it can be observed that there is a redshift in resonant wavelength and the transmissive intensity and the loss both ascend significantly. The wavelengths of dip A shift from 1378.4 nm to 1397.6 nm, respectively, totaling 19.2 nm, the contrast changes 10.286 dB from -35.806 dB to -25.52 dB. And the wavelengths of dip B are shifted from 1483.8 nm to 1503.2 nm, respectively, and total is 19.4 nm, the contrast changes 2.311 dB from -41.42 dB to -39.109 dB. When the CLPFGs is wrapped in MF, the refractive index of external environment changes, which results in spectral characteristics of the CLPFGs.

Figure 4
(a) Magnetic field characterization of the initial CLPFGs before packaged
(b) Transmission spectra of the magnetic field sensors before and after MF packaged

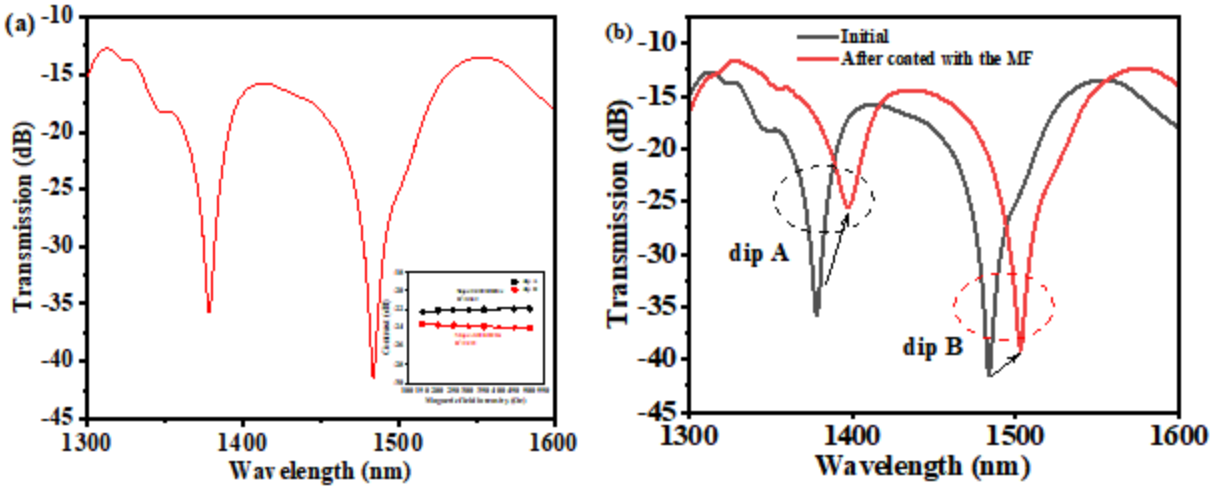

The transmission spectra of CLPFGs with an 8.5mm grating length shift when magnetic field intensity changes, as displayed in Figure 5(a). The two resonant dips can be seen to steadily develop as magnetic field strength increases. As the surrounding magnetic field increases from 150 to 500 Oe, the transmissive intensities of the dip A increased from -24.599 dB to -23.517 dB and dip B increased from -35.999 dB to -30.048 dB, respectively. The external magnetic field causes magnetization of Fe_3O_4 nanoparticles on the CLPFGs structure and the generated magnetostrictive strain leads to the strain optical effect of CLPFGs. And the structure of the CLPFGs is affected by magnetostrictive strain, the refractive index of entire grating region changes (Wang & Chiang, 2015). Figure 5(b) displays the relationship of transmissive intensity of two resonant dips on magnetic field variations. The magnetic field sensitivities of dip A and dip B obtained through linear fitting are 0.003 dB/Oe and 0.017 dB/Oe, respectively. When the resonant dip has larger transmissive depth, it presents faster descend to external magnetic field, resulting in higher sensitivity.

Figure 5
(a) Measured spectra with various magnetic field intensities of the 8.5 mm-length CLPFGs MFS (b) Relationship between the resonant dips and magnetic field intensity

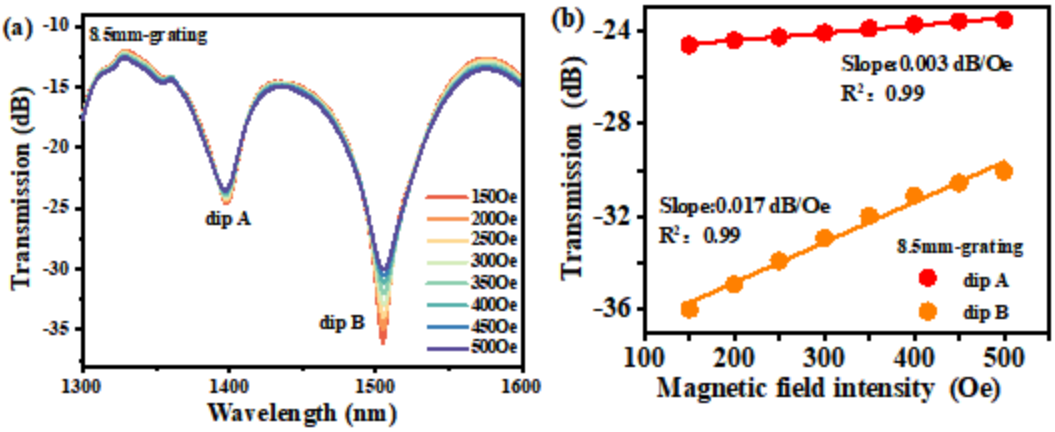

Due to the transmissive and coupling properties of initial CLPFGs (Zhao et al., 2023), the grating length could influence the sensing behaviors, so the magnetic field sensing characteristics of CLPFGs with different lengths were further studied. Figure 6(a) displays the transmission spectrum response of MF-coated CLPFGs with grating length of 9 mm on the surrounding magnetic field increases. The coupling depth of dip A in 9mm-CLPFGs is greater than that of dip B. It has different coupling efficiency with the resonant inclination angle of 8.5mm-CLPFGs. And the dip B is around 1600nm, which is higher order cladding mode and have a higher sensitivity (Zhao et al., 2023). Figure 6(b) illustrates the relationship between the resonant dips and magnetic field intensity, which exhibits the similar magnetic field sensing characteristics as 8.5 mm-length CLPFGs. As the surrounding magnetic field rises from 150 to 500 Oe, the transmissive intensities of dip A and dip B increased. However, when the magnetic field intensity exceeds 220Oe, the magnetic field reaches a saturation state, and the magnetostrictive effect decreases which results the transmission loss changes gradually decrease. As shown in Figure 6(c), we record every minute until the spectrum remains stable, and the average response time of the sensor is approximately 5 minutes.

Figure 6
(a) Measured spectra with various magnetic field intensities of the 9 mm-length CLPFGs MFS (b) Relationship between the resonant dips and magnetic field intensity (c) Determination of the response time of the CLPFGs

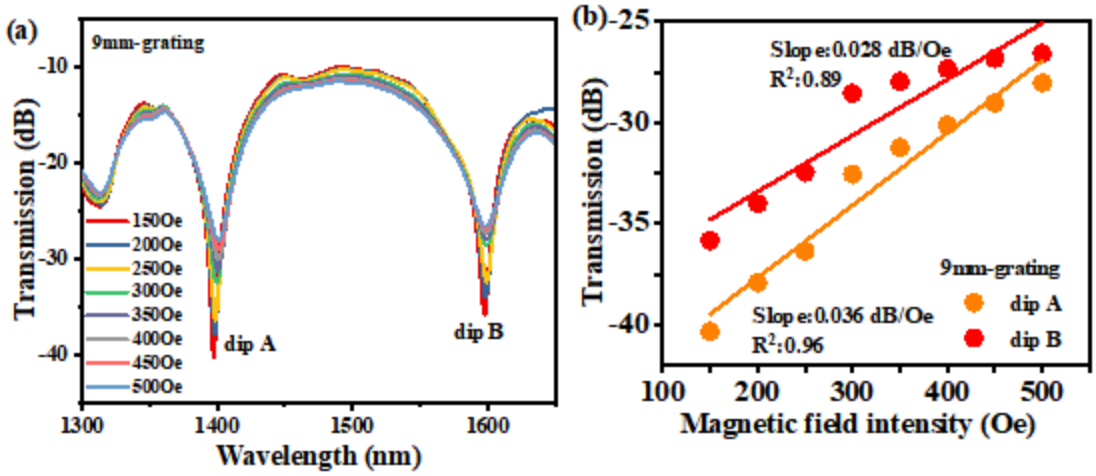

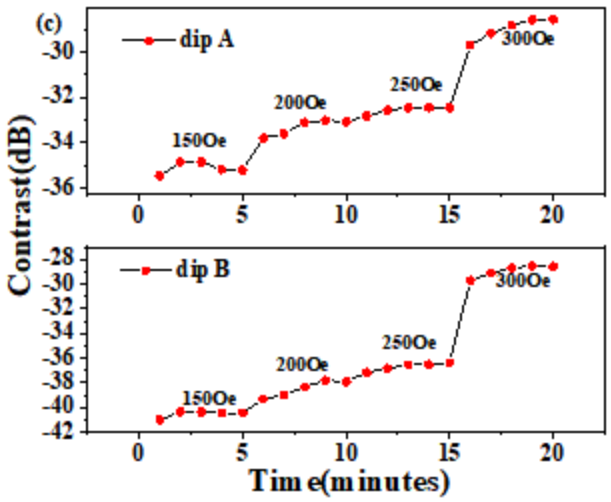

Figure 7(a) displays the transmission spectrum of CLPFGs at different magnetic field intensities when grating length is 10mm. Two resonant dips have been detected at 1552.4 nm (dip A) and 1618.1 nm (dip B), with corresponding contrasts of -29.30 dB and -41.95 dB. As the intensity increases, the resonant wavelength shifts slightly, and the transmissive intensity shows a slow increasing trend. When magnetic field rises from 150 Oe to 500 Oe, the contrast changes are -29.302~-25.543 dB and -41.945~-29.49 dB, respectively. According to Figure 7(b), linear fitting shows that magnetic field sensitivities of dip A and dip B are 0.012 dB/Oe and 0.034dB/Oe, respectively.

Figure 7
(a) Measured spectra with various magnetic field intensities of the 10 mm-length CLPFGs MFS (b) Relationship between the resonant dips and magnetic field intensity

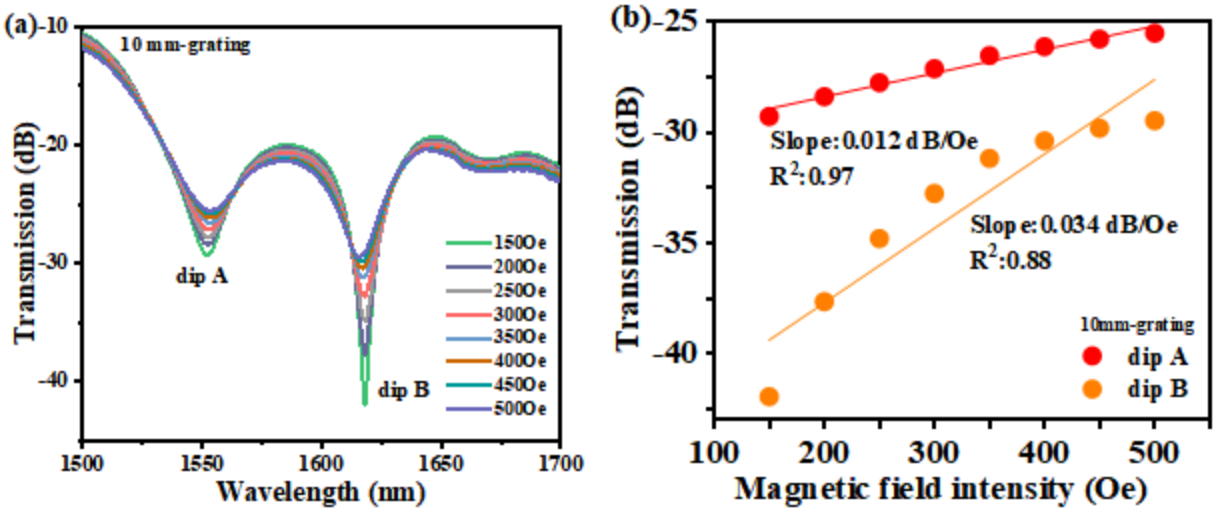

Table 1
Sensitivity comparison of the MFSs with different capillary long period grating structures

	Magnetic field sensitivity (dB/Oe)		Magnetic field range (Oe)
	dip A	dip B	
8.5 mm-CLPFGs	0.003	0.017	150~500
9 mm-CLPFGs	0.028	0.036	150~500
10 mm-CLPFGs	0.012	0.034	150~500

Table 1 shows magnetic field sensitivity of MF-coated CLPFGs with different gratings lengths. LPFGs can perceive changes in optical properties caused by magnetic fields, and their transmission minimum and resonant wavelength are extremely sensitive to changes in surrounding medium. By introducing LPFGs into capillary fibers, the coupling between propagation core mode and cladding mode is promoted. And we can observe that the resonant dip presents faster descend to external magnetic field as larger transmissive depth achieved, which results in higher sensitivity. When the length of the capillary fiber grating is 9mm, the CLPFGs sensor achieves a maximum magnetic field sensitivity of 0.036 dB/Oe.

In addition, the temperature characteristics of the sensor are measured experimentally, as shown in Figure 8. The contrasts of MF-coated CLPFGs sensor do not change significantly with temperature varies. Therefore, the sensor is insensitive to temperature. The temperature cross sensitivity may be disregarded due to the low temperature sensitivity. Compared with other grating-based MFSs, the suggested MF-coated CLPFGs-based MFS could be used to accurately detect the magnetic field strength.

Figure 8
Contrasts variation with the increase of temperature

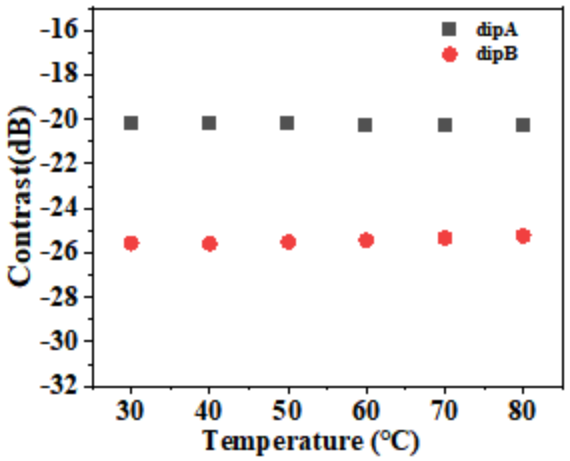

4. Conclusion

In conclusion, we presented a temperature-insensitive MF-coated CLPFGs magnetic field sensor. The CLPFGs were fabricated by arc discharge method and then immersed with the magnetic fluid. The magnetic field sensing characteristics of bare and MF-coated CLPFGs have been investigated experimentally. With MF coating, the magnetic field sensing sensitivity could be enhanced. The experimental results demonstrate that with the increasing external magnetic field, the intensity of resonant dips gradually decreased, which is caused by magnetostrictive effect together with refractive index variations. Moreover, the magnetic field sensing characteristics of CLPFGs with grating lengths of 8.5mm, 9mm and 10mm were studied comparatively. When the grating length of the CLPFGs is 9mm, the sensor can realize a sensitivity of 0.036 dB/Oe. In addition, the presented sensor can measure the magnetic field without temperature cross-sensitivity. The proposed sensor has the advantages of simple structure, low cost and convenient to fabrication performance and exhibits promising application prospects.

Recommendations

The magnetic field sensing research based on magnetic fluid materials and CLPFGs studied in this article is conducted under the condition that the electric field direction of the incident light is perpendicular to the emission direction of the magnetic field. If further research is needed to study changes in magnetic field characteristics under parallel or other angles, further research is needed.

Acknowledgement

This work is jointly sponsored by National Natural Science Foundation of China (62005157), "Chenguang Program" supported by Shanghai Education Development Foundation and Shanghai Municipal Education Commission, and Shanghai Sailing Program (20YF1416800).

Conflicts of Interest

Yunhe Zhao is an associate editor for *Journal of Optics and Photonics Research*, and was not involved in the editorial review or the decision to publish this article. The authors declare that they have no conflicts of interest to this work.

References

Alberto, N., Domingues, M. F., Marques, C., André, P., & Antunes, P. (2018). Optical fiber magnetic field sensors based on magnetic fluid: A review. *Sensors, 18*(12), 4325.

Bao, L., Dong, X., Zhang, S., Shen, C., & Shum, P. P. (2018). Magnetic field sensor based on magnetic fluid-infiltrated phase-shifted fiber Bragg grating. *IEEE Sensors Journal, 18*(10), 4008-4012.

Deng, M., Sun, X., Han, M., & Li, D. (2013). Compact magnetic-field sensor based on optical microfiber Michelson interferometer and Fe3O4 nanofluid. *Applied Optics, 52*(4), 734-741.

Guo, Z., Bai, Y., Zhang, W., Liu, S., Pan, Y., Zhang, X., ..., & Li, X. (2023). Temperature compensated magnetic field sensor based on magnetic fluid infiltrated cascaded structure of micro-tapered long-period fiber grating and fiber Bragg grating. *Sensors and Actuators A: Physical, 358*, 114425.

Hadjigeorgiou, N., Asimakopoulos, K., Papafotis, K., & Sotiriadis, P. P. (2021). Vector magnetic field sensors: Operating principles, calibration, and applications. *IEEE Sensors Journal, 21*(11), 12531-12544.

Hsieh, P. H., & Chen, S. J. (2021). An out-of-plane sensing fluxgate magnetic field sensor with an assisted flux conductor. *AIP Advances, 11*(1), 015217.

Konstantaki, M., Candiani, A., & Pissadakis, S. (2011). Optical fibre long period grating spectral actuators utilizing ferrofluids as outcladding overlayers. *Journal of the European Optical Society-Rapid publications, 6*.

Li, P., Yan, H., Xie, Z., Li, Y., & Zhao, X. (2020). An intensity-modulated and large bandwidth magnetic field sensor based on a tapered fiber Bragg grating. *Optics & Laser Technology, 125*, 105996.

Lu, K., Jiang, C., Mou, C., Liu, Y., Wang, H., & Zhu, Y. (2022). High-sensitivity magnetic field sensor based on long-period grating near the dispersion turning point. *IEEE Sensors Journal, 22*(14), 14109-14117.

Luo, Y., Lei, X., Shi, F., & Peng, B. (2018). A novel optical fiber magnetic field sensor based on Mach-Zehnder interferometer integrated with magnetic fluid. *Optik, 174*, 252-258.

Mihailovic, P., & Petricevic, S. (2021). Fiber optic sensors based on the Faraday effect. *Sensors, 21*(19), 6564.

Murzin, D., Mapps, D. J., Levada, K., Belyaev, V., Omelyanchik, A., Panina, L., & Rodionova, V. (2020). Ultrasensitive magnetic field sensors for biomedical applications. *Sensors, 20*(6), 1569.

Poliakov, S. V., Reznikov, B. I., Shchennikov, A. V., Kopytenko, E. A., & Samsonov, B. V. (2017). The range of induction-coil magnetic field sensors for geophysical explorations. *Seismic Instruments, 53*(1), 1-18.

Roy, A., Sampathkumar, P., & Kumar, P. A. (2020). Development of a very high sensitivity magnetic field sensor based on planar Hall effect. *Measurement, 156*, 107590.

Shao, F., Li, S., Lu, L., Kuai, Y., Cao, Z., Xu, F., ..., & Hu, Z. (2023). High sensitivity and dual parameters micro-tapered-LPG sensor. *Optics and Lasers in Engineering, 164*, 107498.

Tang, J., Pu, S., Luo, L., & Dong, S. (2015). Simultaneous measurement of magnetic field and temperature based on magnetic fluid-clad long period fiber grating. *Journal of the European Optical Society-Rapid publications, 10*.

Tian, P., Guan, C., Ye, P., Cheng, T., Yang, J., Zhu, Z., ..., & Yuan, L. (2022). Dual mode interference magnetic-field sensor based on hollow suspended-core fiber. *IEEE Photonics Technology Letters, 34*(1), 43-46.

Wang, C., Su, W., Hu, Z., Pu, J., Guan, M., Peng, B., ..., & Liu, M. (2018). Highly sensitive magnetic sensor based on anisotropic magnetoresistance effect. *IEEE Transactions on Magnetics, 54*(11), 1-3.

Wang, S. F., & Chiang, C. C. (2015). A micro rectangular-shaped long-period fiber grating coated with Fe3O4 nanoparticle thin overlay for magnetic sensing. *Materials, 8*(10), 7074-7085.

Wang, X. X., Zhao, Y., Lv, R. Q., Zheng, H. K., & Cai, L. (2021). Magnetic field measurement method based on the magneto-volume effect of hollow core fiber filled with magnetic fluid. *IEEE Transactions on Instrumentation and Measurement, 70*, 1-8.

Xu, R., Xue, Y., Xue, M., Ke, C., Ye, J., Chen, M., ..., & Yuan, L. (2022). Simultaneous measurement of magnetic field and temperature utilizing magnetofluid-coated SMF-UHCF-SMF fiber structure. *Materials, 15*(22), 7966.

Yang, D., Du, L., Xu, Z., Jiang, Y., Xu, J., Wang, M., ..., & Wang, H. (2014). Magnetic field sensing based on tilted fiber Bragg grating coated with nanoparticle magnetic fluid. *Applied Physics Letters, 104*(6), 061903.

Yang, M., Dai, J., Zhou, C., & Jiang, D. (2009). Optical fiber magnetic field sensors with TbDyFe magnetostrictive thin films as sensing materials. *Optics Express, 17*(23), 20777-20782.

Zhang, J., Jiang, Y., Chen, H., Zhang, X., Guo, Z., & Wang, W. (2022). Vectorial magnetic field sensing by magnetic-fluid-infiltrated eccentric fiber Bragg grating. *IEEE Sensors Journal, 22*(21), 20508-20515.

Zhang, N. M. Y., Dong, X., Shum, P. P., Hu, D. J. J., Su, H., Lew, W. S., & Wei, L. (2015). Magnetic field sensor based on magnetic-fluid-coated long-period fiber grating. *Journal of Optics, 17*(6), 065402.

Zhang, Y. N., Zhu, N., Gao, P., & Zhao, Y. (2020). Magnetic field sensor based on ring WGM resonator infiltrated with magnetic fluid. *Journal of Magnetism and Magnetic Materials, 493*, 165701.

Zhao, Y., Tang, M., Ma, Y., Liu, Y., Yang, Y., & He, Z. (2023). Fabrication and sensing characteristics of long-period fiber grating in capillary fiber. *IEEE Sensors Journal, 23*(4), 3581-3588.

Zheng, Y., Chen, L. H., Yang, J., Raghunandhan, R., Dong, X., So, P. L., & Chan, C. C. (2017). Fiber optic Fabry–Perot optofluidic sensor with a focused ion beam ablated microslot for fast refractive index and magnetic field measurement. *IEEE Journal of Selected Topics in Quantum Electronics, 23*(2), 322-326.

How to Cite:

Ding, M., Tang, M., Hua, Z., Wang, X. & Zhao, Y. (2023). Magnetic Field Sensing by Magnetic-Fluid-Coated Capillary Long-Period Fiber Gratings. *Journal of Optics and Photonics Research*. https://doi.org/10.47852/bonviewJOPR32021778